LA-UR-09-6258

Approved for public release;
distribution is unlimited.

Title: On the Accuracy of a Common Monte Carlo Surface Flux Grazing Approximation

Author(s): Jeffrey A. Favorite, X-1-TA
Ashley D. Thomas, South Carolina State University
Thomas E. Booth, X-3-MA

Intended for: Nuclear Science and Engineering

On the Accuracy of a Common Monte Carlo Surface Flux Grazing Approximation

Jeffrey A. Favorite*
Computational Physics (X-CP) Division, MS F663
Los Alamos National Laboratory
Los Alamos, NM 87545 USA

Ashley D. Thomas
Dept. of Civil and Mechanical Engineering Technology and Nuclear Engineering, Box 8143
South Carolina State University
Orangeburg, SC 29117 USA

Thomas E. Booth
Computational Physics (X-CP) Division, MS A143
Los Alamos National Laboratory
Los Alamos, NM 87545 USA

*Corresponding author:
fave@lanl.gov
phone (505) 667-7941
fax (505) 665-4479

Submitted to *Nuclear Science and Engineering* on October 5, 2009.
Revision submitted on August 3, 2010.
Second revision submitted on October 4, 2010.

Total number of pages (not including this cover sheet): 37
Number of tables: 1
Number of figures: 11

On the Accuracy of a Common Monte Carlo Surface Flux Grazing Approximation

Jeffrey A. Favorite*
Computational Physics (X-CP) Division, MS F663
Los Alamos National Laboratory
Los Alamos, NM 87545 USA

Ashley D. Thomas
Dept. of Civil and Mechanical Engineering Technology and Nuclear Engineering, Box 8143
South Carolina State University
Orangeburg, SC 29117 USA

Thomas E. Booth
Computational Physics (X-CP) Division, MS A143
Los Alamos National Laboratory
Los Alamos, NM 87545 USA

*Corresponding author: fave@lanl.gov

Abstract — Particle fluxes on surfaces are difficult to calculate with Monte Carlo codes because the score requires a division by the surface-crossing angle cosine, and grazing angles lead to inaccuracies. We revisit the standard practice of dividing by half of a cosine "cutoff" for particles whose surface-crossing cosines are below the cutoff. We concentrate on the flux crossing an external boundary, deriving the standard approach in a manner that explicitly points out three assumptions: (a) that the external boundary surface flux is isotropic or mostly isotropic; (b) that the cosine cutoff is small; and (c) that the minimum possible surface-crossing cosine is 0. We find that the requirement for accuracy of the standard surface flux estimate is more restrictive for external boundaries (a very isotropic surface flux) than for internal surfaces (an isotropic or linearly anisotropic surface flux). Numerical demonstrations involve analytic and semianalytic solutions for monoenergetic point sources irradiating surfaces with no scattering. We conclude with a discussion of potentially more robust approaches.

I. INTRODUCTION

The total particle flux on a surface is calculated in Monte Carlo codes by scoring the weight of each particle crossing the surface divided by the cosine of the angle between the particle trajectory and the surface normal.[1-3] When a particle grazes the surface, the cosine of the surface-crossing angle is small, and the particle's score can be huge, leading to infinite variances[1,3] and tallies that may have difficulty converging. In some practical situations, for a reasonable number of starting particles, both the surface flux tally mean and its variance may be inaccurate.

To circumvent this problem, Clark[1] recommended "exclud[ing] grazing fluxes from the stochastic estimate," replacing them with "an independent estimate of the contribution from grazing angles." However, in Ref. 1, Clark did not derive such an estimate. (Alternatively, Clark suggested, "One can…perhaps extrapolate from the smoothed stochastic estimates of the nongrazing angles.")

The standard estimate of the contribution from grazing angles, which can be inferred from Clark's theoretical analysis, is as follows. Let μ represent the cosine of the surface-crossing angle. Let $0 \le |\mu| \le \varepsilon$, where ε is small, represent the "grazing band" (in the language of Ref. 1). Then the prescription is: When $|\mu| > \varepsilon$, score $1/|\mu|$ as normal, but when $|\mu| \le \varepsilon$, score $2/\varepsilon$. In other words, use $2/\varepsilon$ as an estimate of the expected value of $1/|\mu|$ for grazing angles, defined as angles for which $|\mu|$ is smaller than ε. In the MCNP5 general-purpose Monte Carlo code,[4] for example, whenever $|\mu|$ is less than $\varepsilon = 0.1$, $2/\varepsilon = 20$ is scored instead. In Ref. 3, $\varepsilon = 0.01$ is suggested.

The purpose of this paper is to revisit this historic Monte Carlo practice that allows surface-flux estimates with finite variance. Our interest is specifically in situations in which μ is constrained to a half-space, $0 \le \mu \le 1$; for example, at an external boundary. Clark separately addressed surfaces within a medium and those which are external boundaries, naturally but implicitly assuming for the latter a non-zero angular flux only in the half-space. We will show that the standard estimate requires greater isotropy for fluxes on external boundaries than for fluxes on internal surfaces.

More specifically, we are interested in estimating the flux on an exterior surface due to irradiation from an external source as well as uncollided surface fluxes due to that source. These surface fluxes are important for sensitivity analyses in certain problems in which scattering can be ignored.[5,6] As we will show, this is not the type of problem that Clark envisioned when he wrote his seminal paper, so another goal of this paper is to assess the validity of the standard approximation for these types of problems.

In Sec. II, we provide a derivation of the estimate that complements the derivation given in Ref. 3 and highlights some assumptions. Our derivation allows the identification of several practical situations in which the standard estimate is bound to fail, as well as several practical situations in which the standard estimate is shown to be accurate. Numerical demonstrations, none of which include scattering, are given in Sec. III.

II. DERIVATION AND DISCUSSION OF THE STANDARD ESTIMATE

The particle angular flux $\phi(\mu)$ on a fixed surface is the angular surface-crossing rate $J(\mu)$ divided by the surface-crossing cosine μ (Ref. 3). Following Clark,[1] we expand the surface flux in powers of μ; however, we restrict the range of μ to the half-space:

$$\phi(\mu) = \begin{cases} \dfrac{J(\mu)}{\mu} = \displaystyle\sum_{i=0}^{\infty} g_i \mu^i, & 0 \le \mu \le 1 \\ 0, & -1 \le \mu < 0. \end{cases} \tag{1}$$

The angular surface-crossing rate and thus the flux are zero for particles crossing in the "backward" direction. Thus, in this paper, when we speak of the flux as "isotropic," "linearly isotropic," "nearly isotropic," etc., we (generally) mean in the half-space.

The expected (average) value of $1/\mu$, $\overline{1/\mu}$, for particles sampled on the surface from the function $J(\mu)$ in the half-space for $\mu < \varepsilon$, where ε is small, is

$$\overline{1/\mu} = \frac{\displaystyle\int_{\mu_{min}}^{\varepsilon} d\mu \frac{J(\mu)}{\mu}}{\displaystyle\int_{\mu_{min}}^{\varepsilon} d\mu\, J(\mu)}. \tag{2}$$

In these equations and in the rest of this paper, we assume monoenergetic particles. In Eq. (2), the lower limit of the integrals is μ_{min}, the minimum possible value of the crossing angle cosine, which may be greater than 0 because of geometric limitations. Thus, the actual range of μ may be constrained to be smaller than the half-space. It is also assumed that $\varepsilon > \mu_{min}$. When the expansion of Eq. (1) is used in Eq. (2), the result is

$$\overline{1/\mu} = \frac{\sum_{i=0}^{\infty} \frac{1}{i+1} g_i (\varepsilon^{i+1} - \mu_{min}^{i+1})}{\sum_{i=0}^{\infty} \frac{1}{i+2} g_i (\varepsilon^{i+2} - \mu_{min}^{i+2})}. \quad (3)$$

Clark's analysis[1] retains only two terms in the expansion (g_0 and $g_1 \times \mu$) and assumes "$g_0 \neq 0$ within a medium and $g_1 \neq 0$ at an external boundary." Dupree and Fraley's analysis[3] assumes the flux is "reasonably isotropic." Clark and Dupree and Fraley also assume $\mu_{min} = 0$ always.

From Eq. (3), when the flux is purely isotropic ($g_0 > 0, g_i = 0$ for $i \neq 0$) in the half-space or mostly isotropic ($g_0 >> |g_i|$ for $i \neq 0$) in the half-space and $\mu_{min} = 0$, the expected value is

$$\overline{1/\mu} = \frac{2}{\varepsilon}, \quad (4)$$

as derived in Ref. 3, though not (explicitly) in Ref. 1.

As an aside, we examine the situation when the flux is linearly anisotropic ($g_0 > 0, g_1 \neq 0, g_i = 0$ for $i > 1$) in the full range $-1 \leq \mu \leq 1$ and the grazing band ranges from $-\varepsilon$ to $+\varepsilon$. In this case we use the absolute value of the surface-crossing cosine when relating the angular surface-crossing rate and the flux: $\phi(\mu) = J(\mu)/|\mu|$. Equation (2) becomes

$$\overline{1/\mu} = \frac{\int_{-\varepsilon}^{\varepsilon} d\mu (g_0 + g_1 \mu)}{\int_{-\varepsilon}^{\varepsilon} d\mu (g_0 |\mu| + g_1 \mu |\mu|)}, \quad (5)$$

which also leads to Eq. (4) (the g_1 terms in both the numerator and denominator integrate to zero). This is the basis for the prescription described in Sec. I for estimating the contribution from grazing angles in Monte Carlo codes, using a substitute cosine divisor that is half the "cutoff" value when the flux is at most linearly anisotropic over the full range $-1 \leq \mu \leq 1$.

However, "[f]or situations where $g_0 = 0$ and $g_1 \neq 0$, say at an external boundary" (Ref. 1, p. 238), i.e. when the flux is purely linear (Clark also has $g_i = 0$ for $i > 1$) at an external boundary, circumstances are different. Note that Clark implicitly assumes a linear flux only in the half-space here; otherwise, incoming fluxes would be negative. Under these assumptions, and also assuming $\mu_{min} = 0$, the expected value [from Eq. (3)] is

$$\overline{1/\mu} = \frac{3}{2\varepsilon}. \tag{6}$$

Thus, code users should be cautious when applying the standard approximation of Eq. (4) to external boundaries. It should be noted that the quote above refers to a special case of an external boundary flux; the more general assumption is "$g_1 \neq 0$ at an external boundary" (Ref. 1, p. 237), with no restriction on g_0.

To reiterate, when the surface flux is isotropic or linearly anisotropic ($g_0 > 0, g_1 \neq 0, g_i = 0$ for $i > 1$) in the full range $-1 \le \mu \le 1$ and $\mu_{min} = 0$, the expected value $\overline{1/\mu}$ is given by the usual formula, Eq. (4). However, on an external boundary, or in other situations in which the surface flux is restricted to the half-space $0 \le \mu \le 1$, the expected value $\overline{1/\mu}$ is given by Eq. (3), which reduces to Eq. (4) only when the flux is purely or mostly isotropic (in the half-space) and $\mu_{min} = 0$. Thus, the requirement for accuracy of the standard surface flux estimate is more restrictive for external boundaries (a very isotropic surface flux) than for internal surfaces (an isotropic or linearly anisotropic flux).

In all cases, the expected value given by Eqs. (2) and (3) is a function of μ_{min}. For the problems envisioned by Clark[1] and Dupree and Fraley,[3] particle scattering within materials can lead to very nearly tangent grazing on exterior boundaries,[a] and μ_{min} is essentially 0. This is an implicit assumption. When nearly or exactly tangent grazing is not possible, however, $\mu_{min} > 0$ and Eqs. (4) and (6) are not obtained. Such situations can arise when estimating the surface flux due to an external point source and when uncollided surface fluxes are computed. (In these cases, positive μ is in the direction of the rays, which may be opposite the direction of the outward surface normal for the external boundary.)

Thus, there are many situations in which $2/\varepsilon$ is a poor estimate of $\overline{1/\mu}$.

In some cases, the surface flux cannot be expanded in powers of μ. For example, if the flux has a $1/\mu$ dependence in the half-space, such that

[a] Ref. 3 says that "for convex surfaces on the exterior of a problem geometry to which vacuum boundary conditions are applied, the flux tangent to the surface will be zero." However, extremely small crossing angles may still be obtained.

$$\phi(\mu) = \frac{J(\mu)}{\mu} = g_r \frac{1}{\mu} \tag{7}$$

[where g_r is just a coefficient for the reciprocal-μ dependence and not one of the g_i of Eq. (1)], then the expected value of $1/\mu$ is

$$\overline{1/\mu} = \frac{\int_{\mu_{min}}^{\varepsilon} d\mu\, g_r \frac{1}{\mu}}{\int_{\mu_{min}}^{\varepsilon} d\mu\, g_r} = \frac{\ln \frac{\varepsilon}{\mu_{min}}}{\varepsilon - \mu_{min}}, \tag{8}$$

a function of μ_{min}, as before. But if the minimum possible value of μ is 0, then the expected value of $1/\mu$ is meaningless — and $2/\varepsilon$ is a poor estimate of $\overline{1/\mu}$. Furthermore, if the flux has a $1/|\mu|$ dependence in the whole range $-1 \le \mu \le 1$, integrating over $[-\varepsilon, \varepsilon]$, as is done in Eq. (5), is integrating over a discontinuity at $\mu = 0$. This example obviously violates the standard assumption of a "reasonably isotropic"[3] flux; it is merely cautionary. The surface flux due to an irradiating source may very easily have such a distribution, as shown in the next section.

III. NUMERICAL DEMONSTRATIONS

III.A. Point Source Irradiating a Disk

Consider a point source centered over a disk, as shown in Figure 1. Let the source angular density be $S(\Omega)$ particles per unit solid angle per unit time (time is not necessary but customary; most people think of steady-state problems as "per unit time"). The direction Ω is defined by the polar angle θ, measured from a line connecting the source point with the center of the disk, and the azimuthal angle ω, measured from an arbitrary line through the source point and perpendicular to the line defining θ. See Figure 1. The differential solid angle element is the differential element of surface area on the unit sphere surrounding the source point: $d\Omega = \sin\theta\, d\theta\, d\omega$. The rate of particles emitted into the cone subtending solid angle $d\Omega$ about direction Ω is

$$S(\Omega)d\Omega = S(\theta, \omega)\sin\theta\, d\theta\, d\omega. \tag{9}$$

A similar problem has been worked out previously[7]; we work it out here in order to highlight the points important to the present paper as well as to establish the method and notation for the more difficult problem in the next section.

In an infinite medium that is purely absorbing with cross section Σ, the particle flux ϕ in the cone a distance x from the source is[8] the product of the source rate, an exponential attenuation factor, a geometric attenuation factor (inverse-square law for distance), and $1/4\pi$:

$$\phi(x,\Omega)d\Omega = \frac{S(\Omega)e^{-\Sigma x}}{4\pi x^2}d\Omega. \tag{10}$$

In this paper we let the source angular density depend on the polar angle θ but not the azimuthal angle ω. Thus, we drop the ω argument and use $S(\theta) \equiv S(\theta,\omega)$ and, since the objects of interest and the intervening media will also have no ω dependence, $\phi(x,\theta) \equiv \phi(x,\theta,\omega) = \phi(x,\Omega)$. Using Eq. (9) in Eq. (10), integrating over $0 < \omega < 2\pi$, and multiplying both sides by x^2 yields

$$\phi(x,\theta)dA_S = \frac{1}{4\pi}S(\theta)\frac{e^{-\Sigma x}}{x^2}dA_S, \tag{11}$$

where

$$dA_S = 2\pi x^2 \sin\theta\, d\theta \tag{12}$$

is the differential element of surface area of the ring of thickness $d\theta$ formed by the intersection of the cone of opening angle θ and a sphere of radius x centered at the source point. Integrating Eq. (11) over $0 < \theta < \pi$ would give the total flux on the surface of the sphere surrounding the source, which will hereafter be referred to as the "source sphere," although it must be remembered that the source is only a point.

In this section, we desire to know the total flux on the surface of a disk of radius R centered a distance h from the point source, as shown in Figure 1. The source particle ray of trajectory θ intersects the disk at radius r on the disk. Since there is no scattering, the cosine of the source particle trajectory cos θ is the same as the surface-crossing cosine μ (see Figure 1). For a fixed value of θ, the intersection of the source sphere of radius x and the irradiated disk defines the relationships among θ, μ, x, and r (and the constant h):

$$\mu = \cos\theta = \frac{h}{x} = \frac{h}{\sqrt{r^2 + h^2}}. \tag{13}$$

Specifying that the flux of interest is that on the disk only, the dual argument of ϕ in Eq. (11) can be reduced to a single argument, recognizing that $\phi(\theta)$, $\phi(\mu)$, $\phi(x)$, and $\phi(r)$ refer to the flux at the same point (a ring) on the disk and using the argument to identify the functional form that is intended. With this understanding, and replacing dA_S with the differential element of surface area on the disk dA_D, Eq. (11) becomes, for example,

$$\phi(\mu)dA_D = \frac{1}{4\pi} S(\theta) \frac{e^{-\Sigma x(\mu)}}{x(\mu)^2} dA_D; \tag{14}$$

the argument of ϕ and x can equivalently be r or θ.

The differential element of surface area on the disk is related to the differential element of surface area on the source sphere through

$$dA_D = dA_S / \mu \tag{15}$$

(this statement is proved in Appendix A). Using Eqs. (12) and (13), it can easily be shown (see Appendix A) that

$$dA_D = -\frac{2\pi h^2 d\mu}{\mu^3} \tag{16}$$

(as usual, the negative sign is handled by reversing integration limits as appropriate).

Using Eqs. (16) and (13) in Eq. (14) and integrating over μ, the total flux ϕ_T on the surface of the disk is

$$\phi_T = \frac{1}{2} \int_{\mu_{min}}^{1} d\mu\, S(\theta) \frac{e^{\frac{-\Sigma h}{\mu}}}{\mu}, \tag{17}$$

where the minimum possible surface-crossing cosine is [from Eq. (13)]

$$\mu_{min} = \left[(R/h)^2 + 1 \right]^{-1/2}. \tag{18}$$

The integrand of Eq. (17) is $\phi(\mu)$ on the disk surface. For an isotropic source [$S(\theta) = c$, where c is a normalization constant] in a void ($\Sigma = 0$), the surface flux has a $1/\mu$ dependence where it is non-zero. For a linear cosine source [$S(\theta) = c \cos\theta = c\,\mu$] in a void, the surface flux is isotropic where it is non-zero. For a quadratic cosine source [$S(\theta) = c \cos^2\theta = c\,\mu^2$] in a void, the surface flux is linear where it is non-zero.

At this point we change notation slightly. The parameter ε is the cosine cutoff below which μ is considered a grazing angle cosine; thus, ε becomes μ_{cut}. The reciprocal of $\overline{1/\mu}$ is the appropriate substitute cosine divisor to use when $\mu < \mu_{cut}$; thus, $\mu_{sub} \equiv 1/\overline{1/\mu}$, or, rewriting Eq. (2),

$$\mu_{sub} = \frac{\int_{\mu_{min}}^{\mu_{cut}} d\mu\, \mu\phi(\mu)}{\int_{\mu_{min}}^{\mu_{cut}} d\mu\, \phi(\mu)}. \tag{19}$$

In this notation, the standard surface-flux approximation [Eq. (4)] is $\mu_{sub} = \mu_{cut}/2$ for $\mu < \mu_{cut}$.

Now using Eq. (19) with the integrand of Eq. (17) as $\phi(\mu)$, the appropriate value for μ_{sub} for a point source irradiating a disk is

$$\mu_{sub} = \frac{\int_{\mu_{min}}^{\mu_{cut}} d\mu\, S(\theta)\, e^{\frac{-\Sigma h}{\mu}}}{\int_{\mu_{min}}^{\mu_{cut}} d\mu\, S(\theta) \frac{e^{\frac{-\Sigma h}{\mu}}}{\mu}}. \tag{20}$$

Using h = 1 cm and Σ = 0.01 cm^{-1}, μ_{sub}/μ_{cut} is plotted against the ratio of the disk radius to the source distance, R/h, for various values of μ_{cut} in Figs. 2 through 6. Figures 2 and 3 show results for an isotropic point source in a void and a purely absorbing medium, respectively. Figures 4 and 5 show results for a linear cosine point source in a void and a purely absorbing medium, respectively. Figure 6 shows results for a quadratic cosine point source in a void. (For the void cases, the integrals are simple and analytic. For the attenuating cases, numerical evaluation of exponential integrals is required[9]; the integrals are given in the Appendix B.)

For the isotropic point source in a void, the flux at the disk has a purely $1/\mu$ dependence where it is non-zero. Figure 2 shows the dependence of μ_{sub}/μ_{cut} on both μ_{cut} and μ_{min} (or R/h). As suggested in Sec. II, there is no single value of the ratio that would provide an accurate estimate of the surface flux for any single value of R/h or μ_{cut}. In other words, as R/h increases and there is more and more grazing, the appropriate value of μ_{sub}/μ_{cut} changes. Contrast this behavior with that of Figure 3 for an isotropic point source in an attenuating (purely absorbing) medium. As R/h increases, each particular choice of μ_{cut} converges to a specific appropriate value of μ_{sub}/μ_{cut}. Until convergence, however, μ_{sub}/μ_{cut} is a function of μ_{min} (R/h) as in Figure 2. Note, in both Fig. 2 and 3, that the historic value of μ_{sub}/μ_{cut} = ½ has no significance whatsoever.

For the linear cosine point source [$S(\theta) = c \cos\theta = c\,\mu$] in a void, the flux at the disk is purely isotropic where it is non-zero. As derived in Sec. II, the historic value of μ_{sub}/μ_{cut} = ½ is appropriate in this case, but only when μ_{min} is small (large R/h) compared to μ_{cut} [ε in Eq. (3)]. Figure 4 demonstrates this behavior and shows the dependence on μ_{min} and μ_{cut} when μ_{min} is

large (small R/h) compared to μ_{cut}. [From Eq. (18), note that $\mu_{min} \approx h/R$ for $R/h \gtrsim 10$.] In fact, for an isotropic flux, the correct value of the ratio [using Eq. (20) for μ_{sub}] is

$$\frac{\mu_{sub}}{\mu_{cut}} = \frac{1}{2}\left(1 + \frac{\mu_{min}}{\mu_{cut}}\right), \tag{21}$$

which reduces to μ_{sub}/μ_{cut} = ½ when μ_{min}/μ_{cut} is small.

However, Figure 5 for the linear cosine point source in an attenuating medium shows the same behavior as Figure 3: μ_{sub}/μ_{cut} converges to a specific value for a particular choice of μ_{cut}, and the historic value of μ_{sub}/μ_{cut} = ½ has no significance.

For the quadratic cosine point source [$S(\theta) = c \cos^2\theta = c\,\mu^2$] in a void, the flux at the disk is purely linearly anisotropic where it is non-zero. As derived in Sec. II, the historic value of μ_{sub}/μ_{cut} = ½ is not appropriate in this case. Figure 6 demonstrates this. The appropriate value is μ_{sub}/μ_{cut} = ⅔ [Eq. (6)], but only for small μ_{min} (large R/h) relative to μ_{cut}; otherwise, μ_{sub}/μ_{cut} is a function of μ_{min} and μ_{cut}. In fact, for a linear cosine flux, the correct value of the ratio [using Eq. (20) for μ_{sub}] is

$$\frac{\mu_{sub}}{\mu_{cut}} = \frac{2}{3}\left[\frac{1 + (\mu_{min}/\mu_{cut}) + (\mu_{min}/\mu_{cut})^2}{1 + (\mu_{min}/\mu_{cut})}\right]. \tag{22}$$

Although this section deals with an analytic ray-tracing problem, the conclusions apply to the case of the flux on an external boundary enclosing a scattering material. In that situation, μ_{min} is zero, corresponding to very large values of R/h. If the surface flux has a $1/\mu$ dependence or if it is mostly anisotropic, the standard surface flux approximation will not be accurate. If the surface flux is mostly isotropic, the standard surface flux approximation will be accurate.

III.B. Point Source Irradiating a Hollow Sphere

For the case of a point source irradiating a finite disk, when there is no scattering, μ_{min} never quite reaches zero. When an unobstructed point source irradiates a complete sphere, however, μ_{min} does reach zero.

We desire to know the total flux on the surface of a hollow sphere of radius R located a distance h through a void from a point source, as shown in Figure 7. The source is the same as in Sec. III.A; thus, we begin with Eqs. (11) and (12), with $\Sigma = 0$. In this geometry, the cosine of the source particle trajectory $\cos\theta$ is *not* the same as the surface-crossing cosine μ. For a fixed value

of θ, the intersection of a source sphere of radius x and the irradiated sphere defines the relationships among θ, μ, and x (and the constants R and h); x is the distance from the source point along the trajectory θ to the irradiated sphere. As in Sec. III.A, specifying that the flux of interest is that on the irradiated sphere only, the dual argument of ϕ in Eq. (11) can be reduced to a single argument. Equation (11) becomes, for example,

$$\phi(\theta)dA_I = \frac{1}{4\pi}S(\theta)\frac{dA_I}{x(\theta)^2}, \tag{23}$$

using $\Sigma = 0$ and replacing dA_S with the differential element of surface area on the irradiated sphere dA_I.

The differential element of surface area on the irradiated sphere is related to the differential element of surface area on the source sphere through

$$dA_I = dA_S / \mu(\theta) \tag{24}$$

(this statement is proved in Appendix C). Using Eq. (12) in Eq. (24),

$$dA_I = \frac{2\pi\, x(\theta)^2 \sin\theta\, d\theta}{\mu(\theta)}. \tag{25}$$

Using Eq. (25) in Eq. (23) and integrating over θ, the total flux on the surface of a hollow sphere due to a point source in a void is[10]

$$\phi_T = \frac{1}{2}\int_0^{\theta_{max}} d\theta \sin\theta \frac{S(\theta)}{\mu(\theta)}. \tag{26}$$

At θ_{max} the line of length x is tangent to the irradiated sphere. As shown in Appendix C, Eq. (26) can be written in terms of μ as

$$\phi_T = \frac{1}{2}\int_0^1 d\mu \frac{S(\theta)}{\frac{h}{R}\sqrt{\left(\frac{h}{R}\right)^2 + \mu^2 - 1}}. \tag{27}$$

The lower limit of the integral is $\mu_{min} = 0$.

The integrand of Eq. (27) is $\phi(\mu)$ on the surface of the irradiated sphere. For a cosine source,

$$S(\theta) = c\cos\theta = c\frac{R}{h}\sqrt{\left(\frac{h}{R}\right)^2 + \mu^2 - 1} \tag{28}$$

(see Appendix C) and the surface flux is a constant, $\phi(\mu) = c(R/h)^2$. In this case, using Eq. (19), the correct value of μ_{sub}/μ_{cut} is ½ regardless of h and R, since $\mu_{min} = 0$ for all h and R.

For an isotropic source, $S(\theta) = c$, and the flux is a complicated function of μ. Using h = 100 cm, the value of μ_{sub}/μ_{cut} [the numerator is given by Eq. (19)] is plotted against the ratio of the sphere radius to the source distance, R/h, for various values of μ_{cut} in Figure 8. (The integrals are evaluated in Appendix B.) The historic value of μ_{sub}/μ_{cut} = ½ is appropriate in this case for most of the range of R/h and μ_{cut}, except when the source point is very close to the surface of the sphere and μ_{cut} is relatively large. Indeed, the complicated function of μ given by the integrand of Eq. (27) turns out to be surprisingly flat for a large range of R/h.

III.C. Point Source Irradiating a Hollow Rod

A formula for the flux at an external point due to an isotropic cylindrical surface source in a nonattenuating medium is given in Ref. 7. The same formula gives the total flux on the cylindrical surface due to an isotropic point source.[10] The formula involves an incomplete elliptic integral of the first kind that was evaluated for this paper using a numerical integration package.[11]

Although hollow and situated in a void, the rod in this problem had dimensions representative of a nuclear reactor fuel rod: a length of 360 cm and a radius R = 0.5 cm. In one case, the point source was centered along the axis and was a distance h = 0.51 cm from the axis for R/h = 0.98. In another case, the point source was centered along the axis and was a distance h = 1.5 cm from the axis for R/h = 0.33.

The total flux on the cylindrical surface was calculated with a version of MCNP5 that was modified to accept μ_{cut} and μ_{sub} as user inputs. (The modified code also prints more digits in the tally relative errors.) The same random number seed was used for all runs.

The absolute value of the relative difference between the Monte Carlo estimates and the exact solution for the cases of R/h = 0.98 and R/h = 0.33 are plotted in Figure 9 and Figure 10, respectively, as a function of μ_{cut}. Like Figs. 2 through 6 and Fig. 8, Figure 9 shows that the most appropriate value of μ_{sub}/μ_{cut} is not a fixed value but a function of μ_{cut}. Comparing Figure 9 and Figure 10 shows that it is also a function of the geometry. In Figure 10, as in most of

Figure 8 for the hollow sphere, the appropriate value of μ_{sub}/μ_{cut} is ½ for small (≤ 0.01) values of μ_{cut} (although for μ_{cut} = 0.0001 and 0.00001, the results were statistically indistinguishable).

III.D. Point Source Irradiating a Material Sphere

Finally, consider a spherical one-group problem with materials but no scattering. The sphere included seven concentric shells and two materials; parameters are given in Table I. The point source was isotropic and 100 cm from the center of the sphere. The problem is to find the total flux on radius 4. (This is essentially the same problem used in Refs. 5 and 10.) The exact solution was obtained using a numerical integration package[11] with an integrand in a form that does not require the division by the surface-crossing cosine.[10]

The total uncollided flux on surface 4 was calculated with a modified version of MCNP5 that computes uncollided fluxes in arbitrary geometries due to point sources.[5] (This version also accepts μ_{cut} and μ_{sub} as user inputs and prints more digits in the tally relative errors.) The same random number seed was used for all runs.

Results are shown in Figure 11. For this surface, R/h = 0.35, and the results of Sec. III.B suggest that, if there were no attenuation, the standard value of μ_{sub}/μ_{cut} = ½ would be the best choice. Does the attenuation in the spheres affect this conclusion, as it did in Sec. III.A (cosine source irradiating a disk with attenuation, Figure 5)? For the largest value of μ_{cut}, the MCNP5 standard value of 0.1, μ_{sub} = 0.045 was the best of the tested values. However, for μ_{cut} = 0.01 and 0.001, the most accurate results were indeed obtained with μ_{sub}/μ_{cut} = ½. For μ_{cut} = 0.0001 and 0.00001, the results were statistically indistinguishable.

This problem shows again that the most appropriate value of μ_{sub}/μ_{cut} can be a function of μ_{cut} and that it is not always ½. On the other hand, it also corroborates the conclusion of Sec. III.B that for spheres with isotropic point sources and R/h not close to 1, μ_{sub}/μ_{cut} = ½ may be generally appropriate, for small values of μ_{cut}. More attenuation than that present in this geometry, however, might affect this conclusion.

IV. SUMMARY AND CONCLUSIONS

In summary, the standard Monte Carlo surface-flux estimator prescription of scoring $1/|\mu|$ for $|\mu| > \mu_{cut}$ but otherwise scoring $1/\mu_{sub} = 2/\mu_{cut}$ is based on expanding the surface flux in powers of μ and making certain assumptions. Because of Clark's analysis,[1] it is assumed that the flux is isotropic or linearly anisotropic. However, for external boundaries or other surfaces on which crossing is in only one direction, a linearly anisotropic (in the half-space $0 \le \mu \le 1$) flux requires a different score, $1/\mu_{sub} = 3/(2\mu_{cut})$. The standard estimate, which is used in MCNP5 and other Monte Carlo codes, requires greater isotropy for fluxes on external boundaries than for fluxes on internal surfaces.

It is also assumed, but only implicitly in Refs. 1 and 3, that exactly tangent grazing is always possible. However, in streaming problems, this assumption may not be valid. The appropriate estimate then depends on the minimum possible grazing cosine. In fact, this paper shows that for a point source irradiating a finite flat surface, the applicability of the standard $\mu_{sub}/\mu_{cut} = ½$ is actually a rather special case. However, we have found that, for isotropic point sources irradiating curved surfaces, the surface flux is surprisingly isotropic (if the source is not too close to the surface) and $\mu_{sub}/\mu_{cut} = ½$ may be appropriate, even if there is some attenuation.

Finally, it is assumed that the cosine cutoff μ_{cut} is small. This paper has demonstrated this requirement in streaming problems, but it has also demonstrated that the appropriate estimate μ_{sub}/μ_{cut} may in fact depend on μ_{cut}.

The test problems in this paper had streaming and absorption only, no scattering. Whether the flux on an external boundary adjacent to a material with scattering is sufficiently isotropic to allow Eq. (4) to accurately approximate Eq. (3) depends on the specifics of the problem, including, of course, the degree of anisotropic scattering in the material.

Of course, it would be better to develop an approach to the surface-flux problem that did not rely on advance knowledge of the problem-specific parameters μ_{cut} and μ_{sub}. High variance estimators in Monte Carlo transport can often be replaced by lower variance estimators that score on a pseudoparticle that is not part of the particle's random walk. That is, the pseudoparticle is only used for estimation purposes, has no statistical weight for the random walk, and is discarded after the estimate is made. Typically the pseudoparticle is sampled from a biased density that favors sampling of high (unweighted) scores. Because the density is biased to be high where the

(unweighted) score is high, the high score regions are sampled more often, but with reduced weight, so that the variance in the weighted score is much smaller than the variance with an analog estimator. For example, Kalos[12] makes a point detector estimate have finite variance by sampling a pseudoparticle whose collision point is sampled from a biased density that emphasizes collisions close to the point detector. The authors are unaware of any pseudoparticle methods developed for the surface flux grazing angle problem, however.

Another sampling possibility that usually turns infinite variance transport estimates into finite variance estimates is the "ex post facto" method.[13,14] This method has not been tried on the grazing angle problem, but it does convert the infinite-variance point detector estimate into an unbiased finite-variance point detector estimate.[13,14]

Finally, the kernel density estimator has recently been combined with a variance reduction method to estimate the surface flux.[15] The method requires storing all surface crossings with $|\mu| < \mu_{cut}$; their distribution is analyzed in post-processing. Preliminary results for a simple test problem are promising,[15] though a proof of unbiasedness for a finite number of starting particles has not been published.

ACKNOWLEDGMENT

The authors wish to thank Pam Paine (Los Alamos National Laboratory) for drawing Figs. 1 and 7.

APPENDIX A

DISK SURFACE GEOMETRY

We seek to relate the differential element of surface area on the irradiated disk in Figure 1 to the differential element of surface area on a sphere that surrounds the source (the "source sphere") and intersects the disk at radius r on the disk and radius x on the sphere. The source is centered a distance h over the disk. Because there is no scattering, the surface-crossing cosine μ is the same as the cosine of the source trajectory angle θ,

$$\mu = \cos\theta, \tag{29}$$

and, from Figure 1,

$$\mu = \frac{h}{x} = \frac{h}{\sqrt{r^2 + h^2}}. \tag{30}$$

Using Eq. (29),

$$\frac{d\mu}{d\theta} = -\sin\theta. \tag{31}$$

Using Eq. (30),

$$\frac{d\mu}{dr} = -\frac{r\,\mu^3}{h^2}. \tag{32}$$

Therefore, using Eqs. (31) and (32),

$$\begin{aligned} \frac{dr}{d\theta} &= \frac{d\mu}{d\theta} \Big/ \frac{d\mu}{dr} \\ &= \frac{h^2 \sin\theta}{r\,\mu^3}. \end{aligned} \tag{33}$$

Now rearrange Eq. (33) and use $x = h/\mu$ from Eq. (30) to find

$$r\,dr = \frac{1}{\mu}\left(x^2 \sin\theta\, d\theta\right), \tag{34}$$

proving that the differential surface area element on the irradiated disk [the left side of Eq. (34)] is the differential surface area element on the source sphere (the quantity in parentheses on the right side) divided by μ. Multiply Eq. (34) by 2π to get the surface area of the ring.

Now rearrange Eq. (32) to find

$$r\,dr = -\frac{h^2}{\mu^3}\,d\mu. \tag{35}$$

The negative sign in Eq. (35) is handled by reversing the limits of the integration over μ. That is, as θ goes from 0 to its maximum value θ_{max}, μ goes from 1 to its minimum value μ_{min}; the negative sign goes away once the μ integration is made to go from μ_{min} to 1.

APPENDIX B

EVALUATIONS OF INTEGRALS

For completeness, certain integrals used in evaluating Eq. (19) numerically in the test problems are given here. These integrals were obtained using a powerful analytic integrator[16] (essentially a vast integral table) available on the World Wide Web.

The necessary integrals to obtain μ_{sub} for an isotropic or linear cosine point source centered a distance h over a disk of radius R in a purely absorbing (with attenuation coefficient Σ) medium are

$$\int_{\mu_{min}}^{\mu_{cut}} d\mu \, \frac{e^{\frac{-\Sigma h}{\mu}}}{\mu} = \left[E_1\left(\frac{\Sigma h}{\mu}\right) \right]_{\mu_{min}}^{\mu_{cut}}, \tag{36}$$

$$\int_{\mu_{min}}^{\mu_{cut}} d\mu \, e^{\frac{-\Sigma h}{\mu}} = \left[\mu e^{\frac{-\Sigma h}{\mu}} - \Sigma h E_1\left(\frac{\Sigma h}{\mu}\right) \right]_{\mu_{min}}^{\mu_{cut}}, \tag{37}$$

and

$$\int_{\mu_{min}}^{\mu_{cut}} d\mu \, \mu e^{\frac{-\Sigma h}{\mu}} = \frac{1}{2}\left[\mu^2\left(1 - \frac{\Sigma h}{\mu}\right) e^{\frac{-\Sigma h}{\mu}} + (\Sigma h)^2 E_1\left(\frac{\Sigma h}{\mu}\right) \right]_{\mu_{min}}^{\mu_{cut}}, \tag{38}$$

where E_1 is the standard exponential integral function. When $\mu_{cut} = 1$, Eqs. (36), (37), and (38) are used in the equation for the total flux on the disk due to a point source that is isotropic, linear, and quadratic (in μ), respectively. The integrals for the void case ($\Sigma = 0$) are trivial.

The integral in Eq. (36) does not look like the standard E_1 function. To clarify, we here work out Eq. (35) analytically. Let

$$u = \frac{\Sigma h}{\mu}. \tag{39}$$

Then

$$du = -\frac{\Sigma h}{\mu^2} d\mu, \tag{40}$$

leading to [using $\Sigma h = u\mu$ from Eq. (39)]

$$d\mu = -\frac{\mu}{u} du. \tag{41}$$

Define

$$u_1 \equiv \Sigma h/\mu_{min} \text{ and } u_2 \equiv \Sigma h/\mu_{cut}. \tag{42}$$

Using Eqs. (39), (41), and (42), the left side of Eq. (36) becomes

$$\begin{aligned}\int_{\mu_{min}}^{\mu_{cut}} d\mu \frac{e^{\frac{-\Sigma h}{\mu}}}{\mu} &= -\int_{u_1}^{u_2} du \frac{e^{-u}}{u} \\ &= -\left[\int_{u_1}^{\infty} du \frac{e^{-u}}{u} - \int_{u_2}^{\infty} du \frac{e^{-u}}{u}\right] \\ &= -\left[E_1(u_1) - E_1(u_2)\right].\end{aligned} \tag{43}$$

The last line of Eq. (43) uses the definition of the exponential integral $E_1(x)$ with $x = u_1$ and $x = u_2$. Using Eq. (42) results in Eq. (36). With Eq. (36) thus verified, Eqs. (37) and (38) can be verified by differentiating the right sides.

The necessary integrals to obtain μ_{sub} for an isotropic point source a distance h from the center of a hollow sphere of radius R in a void are

$$\int_{\mu_{min}}^{\mu_{cut}} d\mu \frac{1}{\sqrt{\left(\frac{h}{R}\right)^2 + \mu^2 - 1}} = \left[\ln\left(\mu + \sqrt{\left(\frac{h}{R}\right)^2 + \mu^2 - 1}\right)\right]_{\mu_{min}}^{\mu_{cut}} \tag{44}$$

and

$$\int_{\mu_{min}}^{\mu_{cut}} d\mu \frac{\mu}{\sqrt{\left(\frac{h}{R}\right)^2 + \mu^2 - 1}} = \left[\sqrt{\left(\frac{h}{R}\right)^2 + \mu^2 - 1}\right]_{\mu_{min}}^{\mu_{cut}}. \tag{45}$$

These equations can easily be verified by differentiating the right sides. For an unobstructed geometry in which the sphere is completely irradiated, $\mu_{min} = 0$. When $\mu_{cut} = 1$, Eq. (44) is used in the equation for the total flux on the sphere.

APPENDIX C

SPHERICAL SURFACE GEOMETRY

We seek to relate the differential element of surface area on the irradiated sphere in Figure 7 to the differential element of surface area on a sphere that surrounds the source (the source sphere with radius x) and intersects the irradiated sphere at radius R on the irradiated sphere and radius x on the source sphere. The source is located a distance h from the center of the irradiated sphere. From Figure 7, using the right triangle in the irradiated sphere,

$$\mu = \frac{\sqrt{R^2 - h^2 \sin^2\theta}}{R} = \frac{h}{R}\sqrt{\left(\frac{R}{h}\right)^2 - \sin^2\theta}, \tag{46}$$

from which we find

$$\sin\theta = \frac{R}{h}\sqrt{1-\mu^2} \tag{47}$$

(the positive roots are taken because $0 < \theta < \pi$).

The next step is to find x in terms of θ. For this we use the Pythagorean Theorem on the largest triangle in Figure 7:

$$h^2 = h^2 \sin^2\theta + \left[x + \sqrt{R^2 - h^2 \sin^2\theta}\right]^2 \tag{48}$$

and rearrange to find

$$x^2 + \left(2\sqrt{R^2 - h^2 \sin^2\theta}\right)x + \left(R^2 - h^2\right) = 0. \tag{49}$$

The solution is

$$x = -\sqrt{R^2 - h^2 \sin^2\theta} \pm \sqrt{-h^2 \sin^2\theta + h^2}. \tag{50}$$

Arguing that x must be nonnegative, we keep the positive sign and rearrange to find

$$\frac{x}{h} = \sqrt{1-\sin^2\theta} - \sqrt{\left(\frac{R}{h}\right)^2 - \sin^2\theta}. \tag{51}$$

The next step is to find $d\alpha/d\theta$. Using the Law of Sines,

$$\frac{\sin\alpha}{x} = \frac{\sin\theta}{R} \tag{52}$$

or, using Eq. (51) for x,

$$\alpha = \text{asin}\left\{\frac{h\sin\theta}{R}\left[\sqrt{1-\sin^2\theta} - \sqrt{\left(\frac{R}{h}\right)^2 - \sin^2\theta}\right]\right\}. \tag{53}$$

The derivative is

$$\frac{d\alpha}{d\theta} = \frac{h}{R}\frac{\cos\theta}{\cos\alpha}\left[\sqrt{1-\sin^2\theta} - \sqrt{\left(\frac{R}{h}\right)^2 - \sin^2\theta} - \frac{\sin^2\theta}{\sqrt{1-\sin^2\theta}} + \frac{\sin^2\theta}{\sqrt{\left(\frac{R}{h}\right)^2 - \sin^2\theta}}\right], \tag{54}$$

where we have identified $\sqrt{1-\sin^2\alpha} = \cos\alpha$ in the denominator. Combining the third and fourth terms in the brackets and using Eq. (51), this simplifies to

$$\frac{d\alpha}{d\theta} = \frac{x}{R}\frac{\cos\theta}{\cos\alpha}\left[1 + \frac{\sin^2\theta}{\sqrt{1-\sin^2\theta}\sqrt{\left(\frac{R}{h}\right)^2 - \sin^2\theta}}\right]. \tag{55}$$

Identifying $\sqrt{1-\sin^2\theta} = \cos\theta$, using Eq. (46), and doing the addition in the brackets, Eq. (55) becomes

$$\frac{d\alpha}{d\theta} = \frac{x}{R}\frac{\cos\theta}{\cos\alpha}\left[\frac{\frac{R\mu}{h}\cos\theta + \sin^2\theta}{\frac{R\mu}{h}\cos\theta}\right]. \tag{56}$$

Next, note from Figure 7 that $\alpha + \theta = \text{acos}\,\mu$ or, rearranging and taking the cosine of both sides,

$$\cos\alpha = \cos(\text{acos}\,\mu - \theta). \tag{57}$$

Applying the addition theorem for cosines and using (from Figure 7) $\sin(\text{acos}\,\mu) = (h\sin\theta)/R$ yields

$$\cos\alpha = \mu\cos\theta + \frac{h}{R}\sin^2\theta. \tag{58}$$

Using this in Eq. (56) and simplifying yields

$$\frac{d\alpha}{d\theta} = \frac{x}{\mu R}. \tag{59}$$

Finally, rearrange Eq. (59) and use Eq. (52) to find

$$R^2 \sin\alpha \, d\alpha = \frac{1}{\mu}\left(x^2 \sin\theta \, d\theta\right), \tag{60}$$

proving that the differential surface area element on the irradiated sphere [the left side of Eq. (60)] is the differential surface area element on the source sphere (the quantity in parentheses on the right side) divided by μ. Multiply Eq. (60) by 2π to get the surface area of the ring.

To convert Eq. (26) to Eq. (27), use Eq. (46) to find

$$\frac{d\mu}{d\theta} = -\left(\frac{h}{R}\right)^2 \frac{\sin\theta\cos\theta}{\mu} \tag{61}$$

and Eq. (47) to find

$$\cos\theta = \frac{R}{h}\sqrt{\left(\frac{h}{R}\right)^2 + \mu^2 - 1}. \tag{62}$$

Thus

$$\sin\theta d\theta = -\frac{\mu d\mu}{\frac{h}{R}\sqrt{\left(\frac{h}{R}\right)^2 + \mu^2 - 1}}. \tag{63}$$

The negative sign in Eq. (63) is handled by reversing the limits of the integration over μ. That is, as θ goes from 0 to θ_{max}, μ goes from 1 to 0; the negative sign goes away once the μ integration is made to go from 0 to 1.

REFERENCES

1. F. H. CLARK, "Variance of Certain Flux Estimators Used in Monte Carlo Calculations," *Nucl. Sci. Eng.*, **27**, 235-239 (1967).

2. A. DUBI, "Monte Carlo Calculations for Nuclear Reactors," *CRC Handbook of Nuclear Reactors Calculations*, Vol. II, Chap. II , Y. RONEN, Ed., CRC Press, Boca Raton, Florida (1986).

3. S. A. DUPREE and S. K. FRALEY, *A Monte Carlo Primer: A Practical Approach to Radiation Transport*, Chap. 7, Kluwer Academic/Plenum Publishers, New York, New York (2002).

4. X-5 MONTE CARLO TEAM, "MCNP–A General Monte Carlo N-Particle Transport Code, Version 5," Chap. 2, Vol. I, LA–UR–03–1987, Los Alamos National Laboratory (April 24, 2003).

5. J. A. FAVORITE, "Surface and Volume Integrals of Uncollided Adjoint Fluxes and Forward-Adjoint Flux Products in Arbitrary Three-Dimensional Geometries Using MCNP," *Trans. Am. Nucl. Soc.*, **101**, 633-635 (2009).

6. K. C. BLEDSOE, J. A. FAVORITE, and T. ALDEMIR, "Using the Levenberg-Marquardt Method for Solutions of Inverse Transport Problems in One- and Two-Dimensional Geometries," submitted to *Nuclear Technology* (2010).

7. A. B. CHILTON, J. K. SHULTIS, and R. E. FAW, *Principles of Radiation Shielding*, Chap. 6, Prentice-Hall, Englewood Cliffs, New Jersey (1987).

8. J. J. DUDERSTADT and L. J. HAMILTON, *Nuclear Reactor Analysis*, Chap. 4, John Wiley & Sons, New York, New York (1976).

9. W. H. PRESS, S. A. TEUKOLSKY, W. T. VETTERLING, and B. P. FLANNERY, *Numerical Recipes in FORTRAN: The Art of Scientific Computing*, 2nd Ed. (reprinted with corrections), Chap. 6, Cambridge University Press (1994).

10. J. A. FAVORITE, K. C. BLEDSOE, and D. I. KETCHESON, "Surface and Volume Integrals of Uncollided Adjoint Fluxes and Forward-Adjoint Flux Products," *Nucl. Sci. Eng.*, **163**, *1*, 73-84 (2009).

11. R. PIESSENS, E. DEDONCKER-KAPENGA, C. UEBERHUBER, and D. KAHANER, *QUADPACK: A Subroutine Package for Automatic Integration*, Springer-Verlag, New York

(1983); available on the Internet at http://people.scs.fsu.edu/~burkardt/f_src/quadpack/quadpack.html; www.netlib.org.

12. M. H. KALOS, "On the Estimation of Flux at a Point by Monte Carlo," *Nucl. Sci. Eng.*, **16**, *1*, 111-117 (1963).

13. T. E. BOOTH, "Ex Post Facto Monte Carlo Variance Reduction," *Nucl. Sci. Eng.*, **148**, *3*, 391-402 (2004).

14. R. R. PICARD and T. E. BOOTH, "Ensuring Finite Moments in Monte Carlo Simulations via Iterated Ex Post Facto Sampling," *Mathematics and Computers in Simulation*, **79**, *7*, 2106-2121 (2009).

15. K. BANERJEE and W. R. MARTIN, "Kernel Density Estimation Method for Monte Carlo Tallies with Unbounded Variance," *Trans. Am. Nucl. Soc.*, **101**, 430-432 (2009).

16. Wolfram Mathematica Online Integrator, integrals.wolfram.com.

List of Tables

List of Figures

Table I. Spherical Material Test Problem

Radius Index	Outer Radius (cm)	Material	Σ (cm^{-1})
1	20.	Void	0.0
2	25.	1	0.4086457
3	30.	Void	0.0
4	35.	1	0.4086457
5	40.	Void	0.0
6	45.	1	0.4086457
7	50.	2	0.1876253

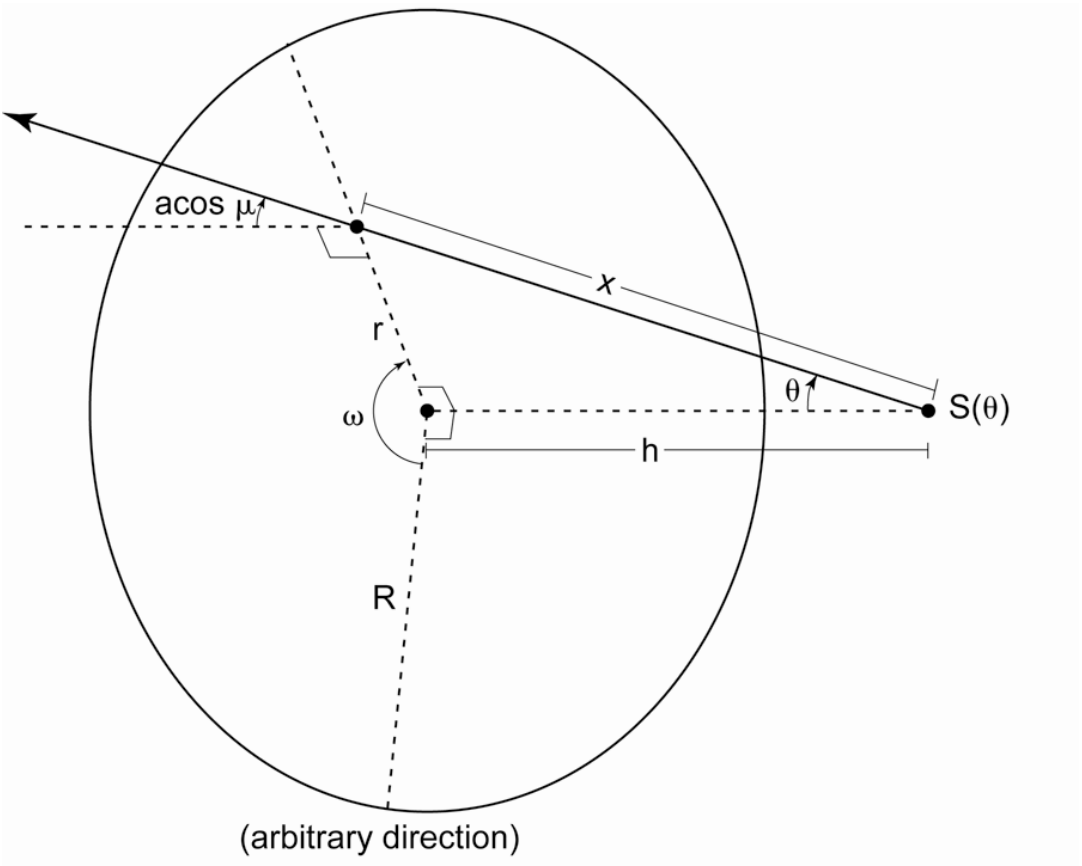

Figure 1. Point source irradiating a disk.

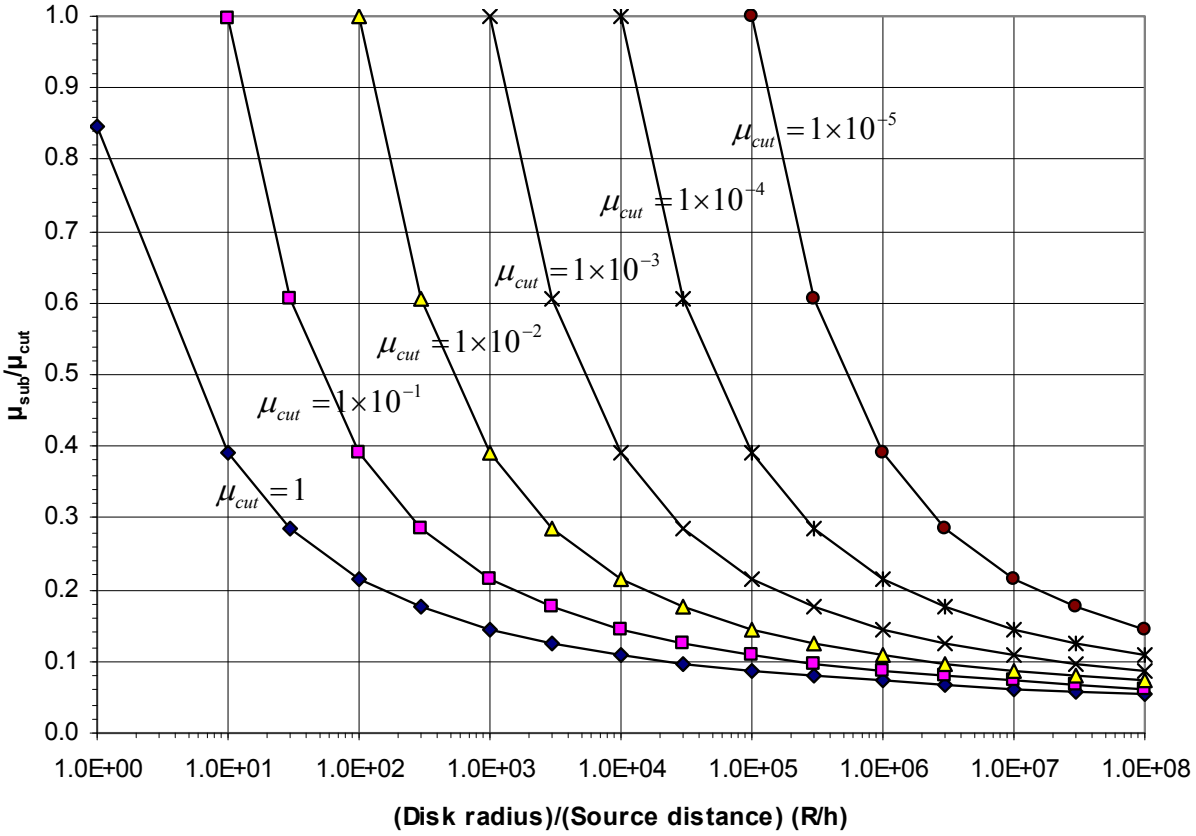

Figure 2. μ_{sub}/μ_{cut} for an isotropic point source irradiating a disk in a void.

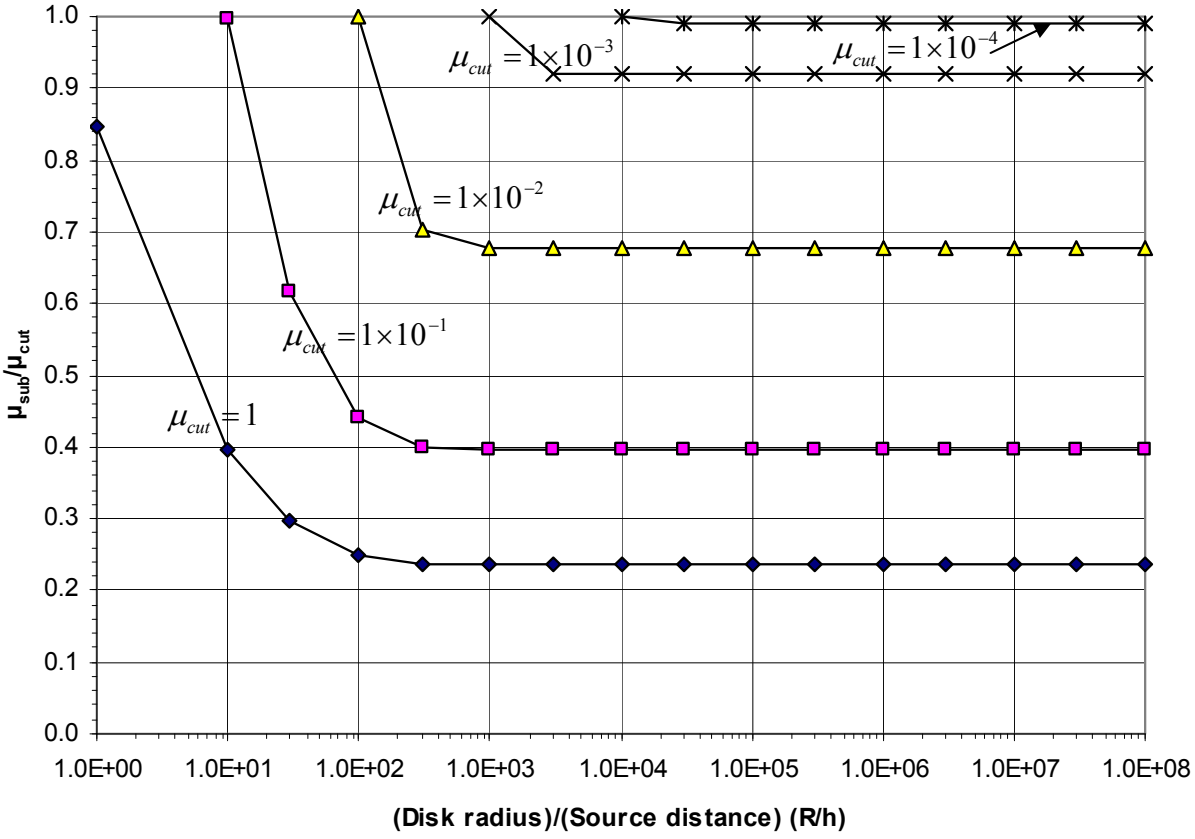

Figure 3. μ_{sub}/μ_{cut} for an isotropic point source irradiating a disk in a purely absorbing medium.

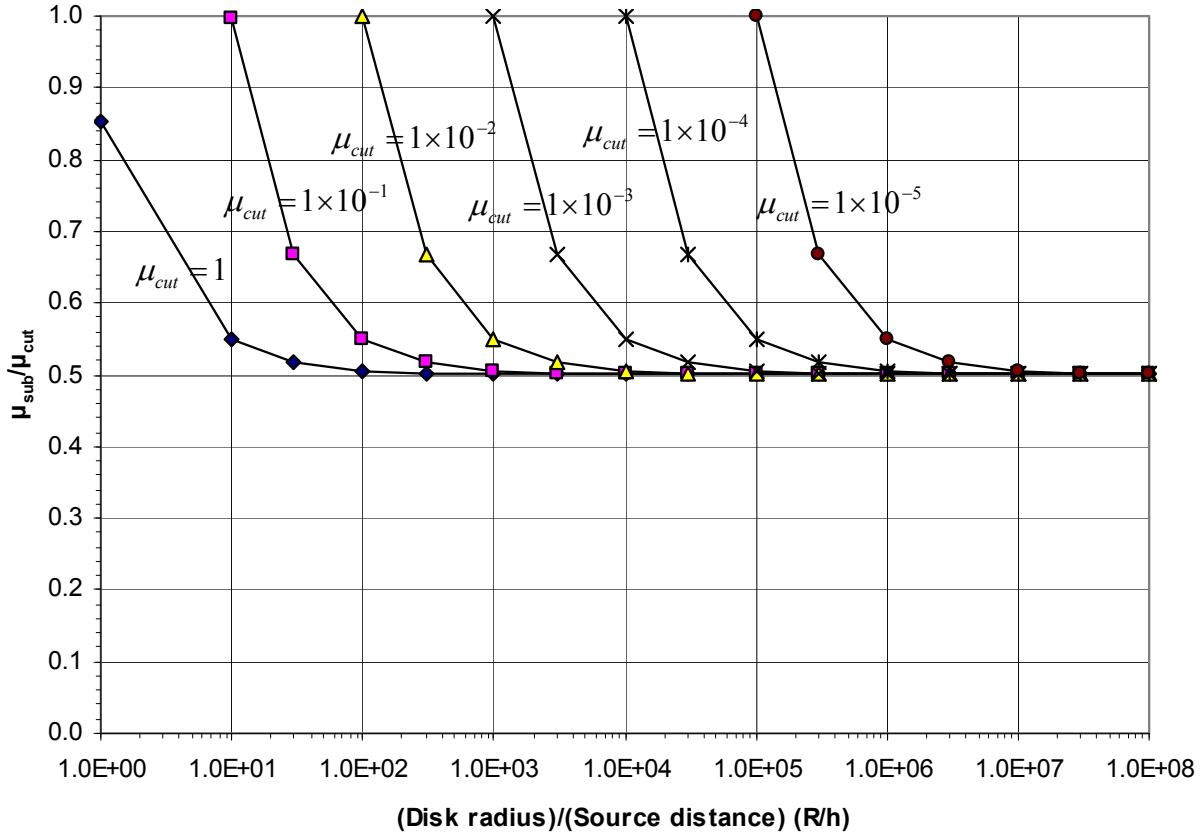

Figure 4. μ_{sub}/μ_{cut} for a linear cosine point source irradiating a disk in a void.

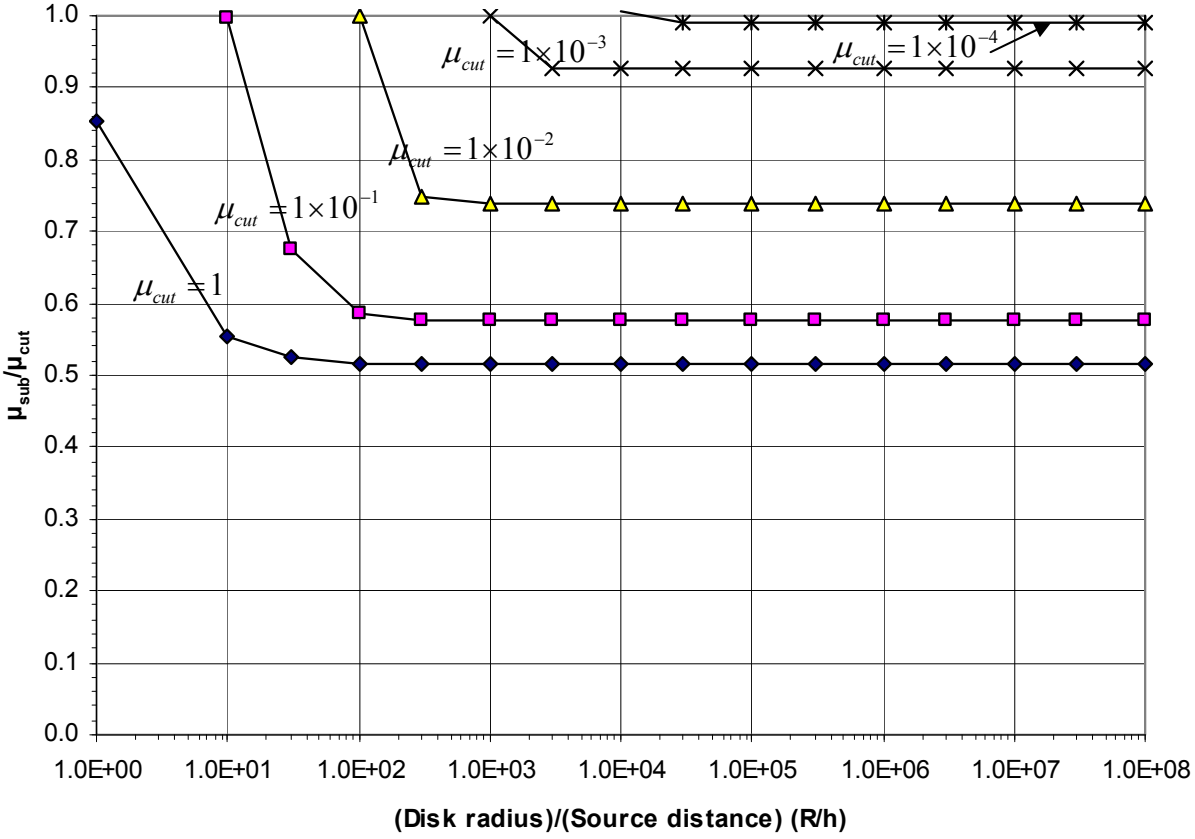

Figure 5. μ_{sub}/μ_{cut} for a linear cosine point source irradiating a disk in a purely absorbing medium.

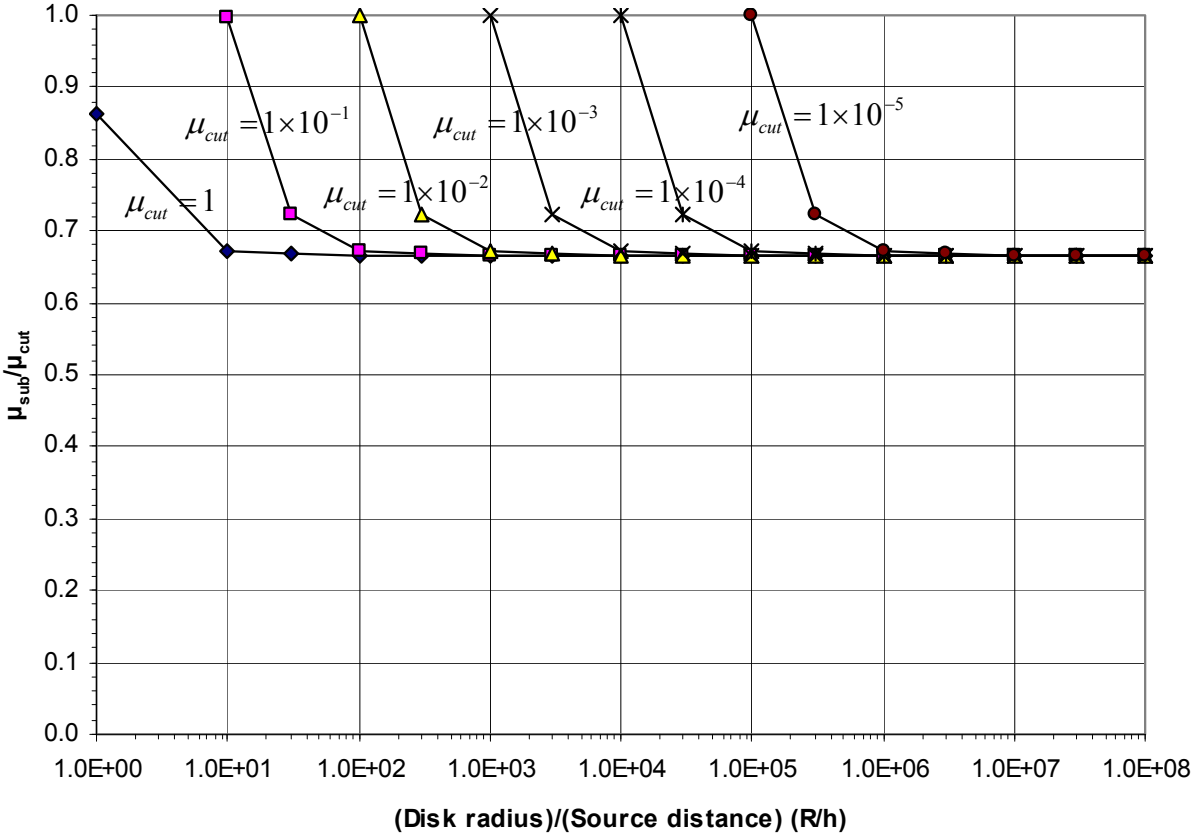

Figure 6. μ_{sub}/μ_{cut} for a quadratic cosine point source irradiating a disk in a void.

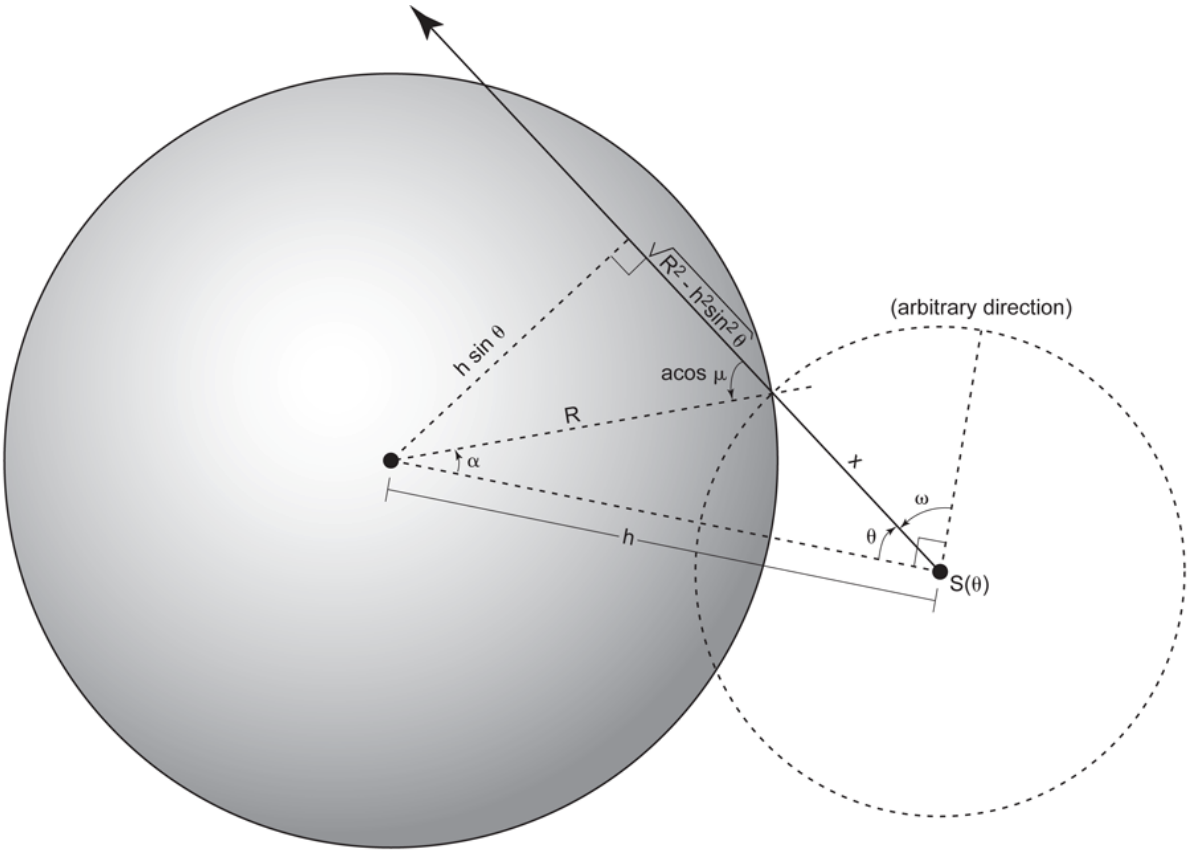

Figure 7. Point source irradiating a sphere.

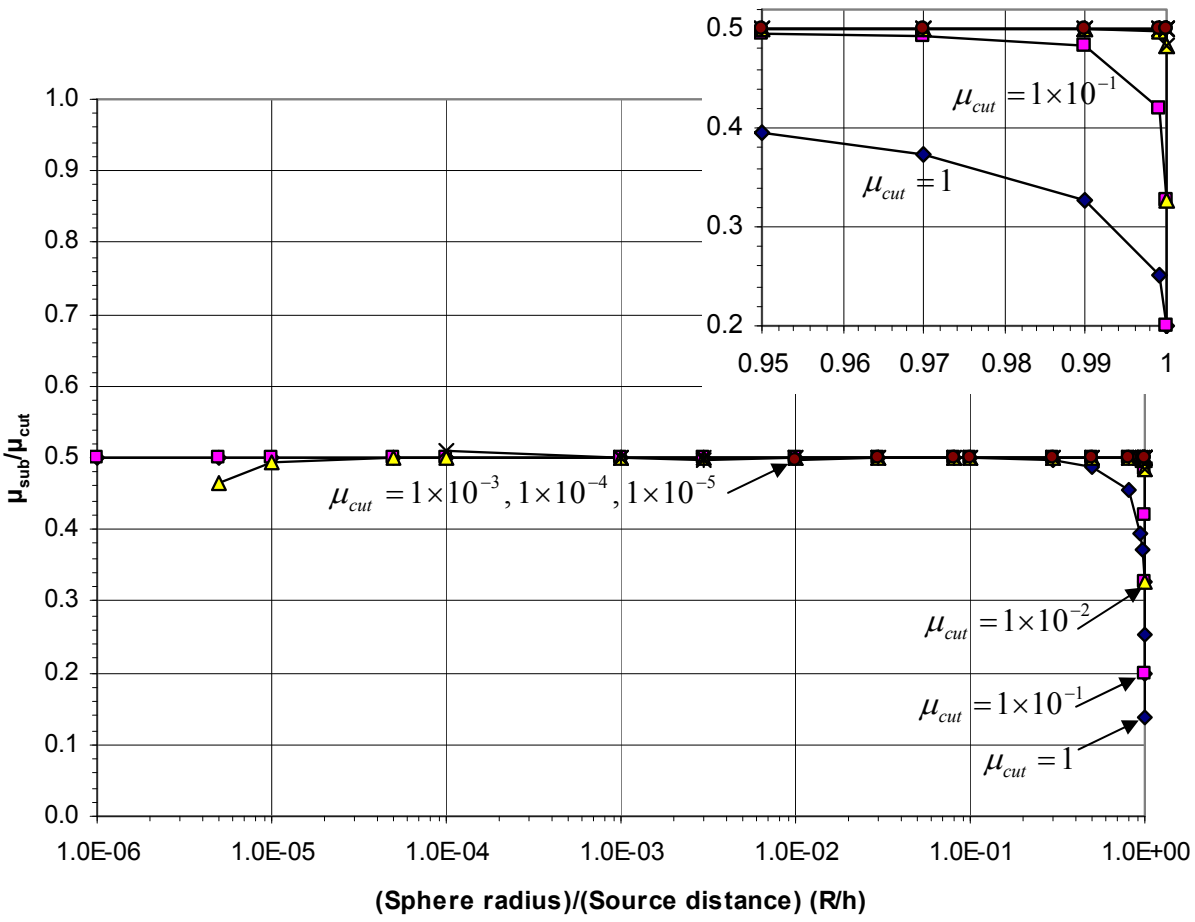

Figure 8. μ_{sub}/μ_{cut} for an isotropic point source irradiating a hollow sphere in a void.

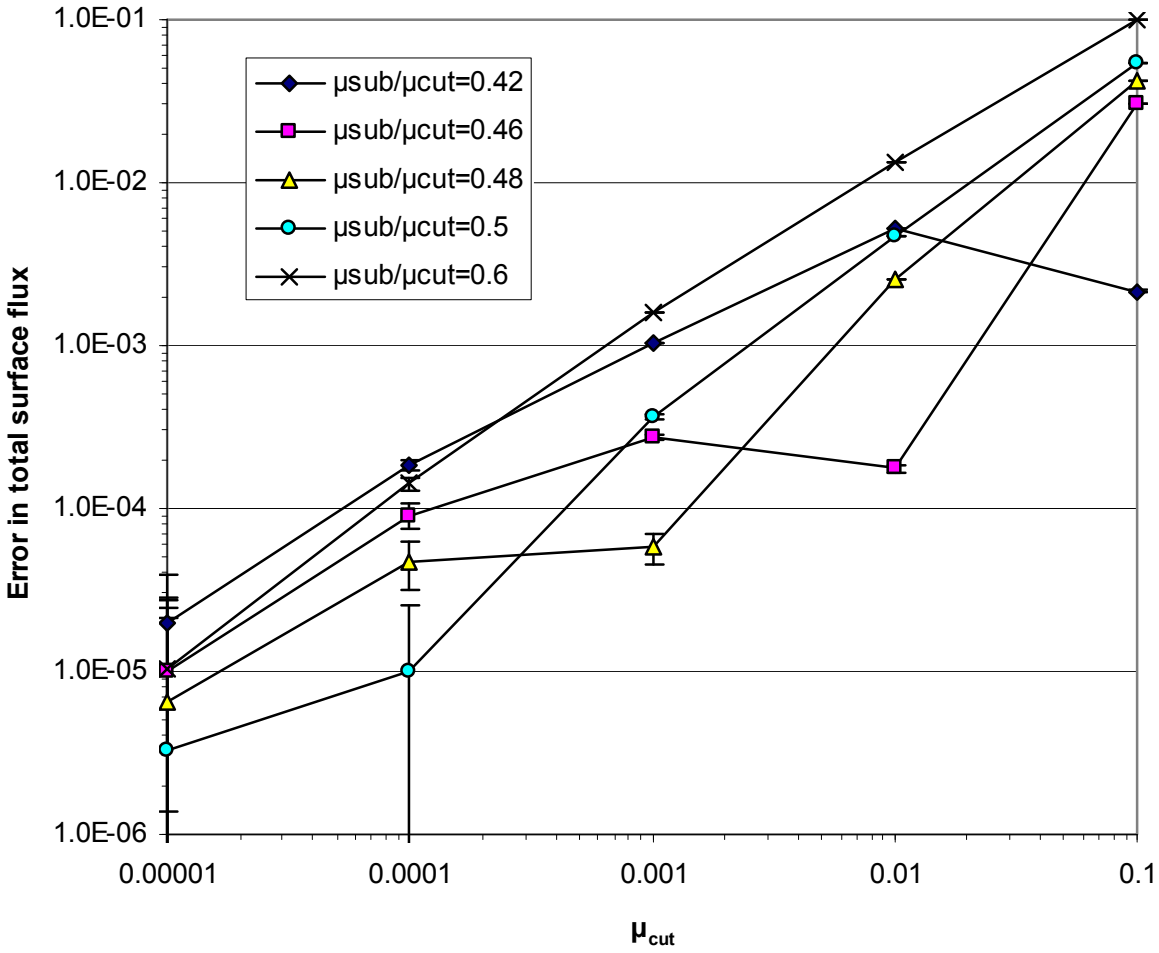

Figure 9. Error in total surface flux on the hollow cylinder with $R/h = 0.98$. Error bars of 1σ are shown.

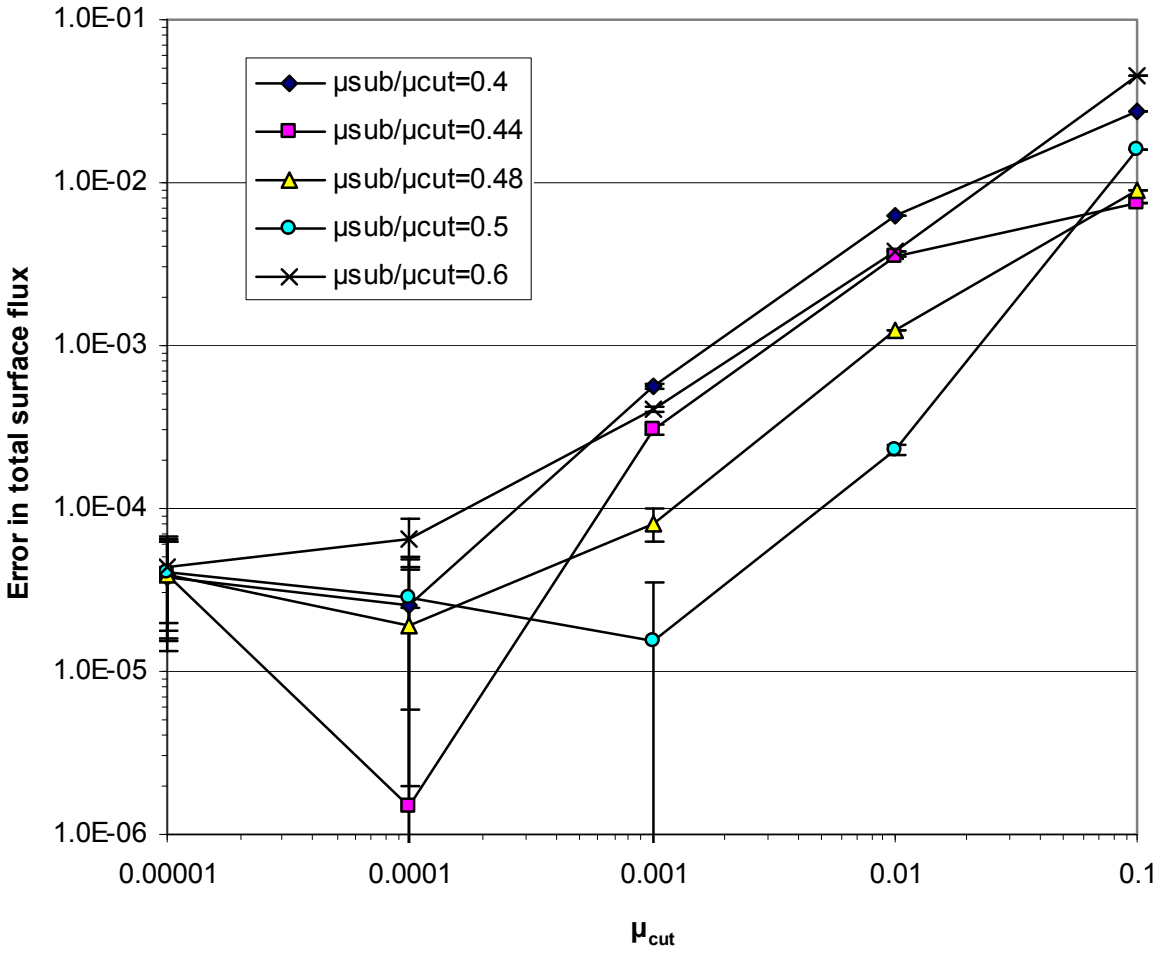

Figure 10. Error in total surface flux on the hollow cylinder with $R/h = 0.33$. Error bars of 1σ are shown.

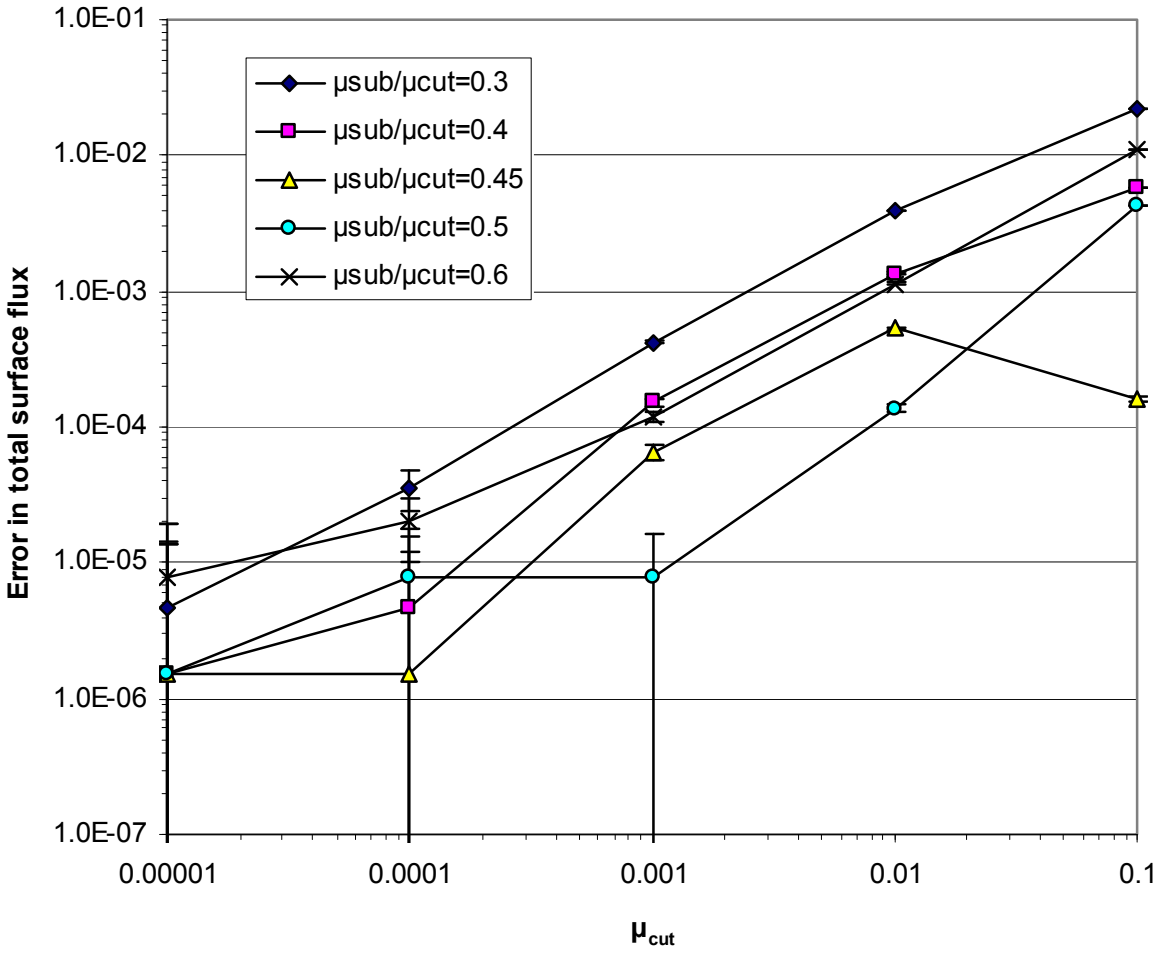

Figure 11. Error in total surface flux on the material spherical shell with $R/h = 0.35$. Error bars of 1σ are shown.